*Plant, Cell & Environment*

WILEY

ORIGINAL ARTICLE

# Xylem Hydraulic Properties of Five *Pinus* Species Grown in Common Environment Vary From Needles to Roots With Needle Length and Native-Range Climate

Na Wang[1,2,3] | Jean-Christophe Domec[2,4] | Sari Palmroth[2] | Christopher A. Maier[5] | Lulu Xie[6,7] | Chunying Yin[6] | Ya-Jun Chen[8] | Ram Oren[2,9]

[1]School of Life Science, Hengyang Normal University, Hengyang, China | [2]Nicholas School of the Environment & Pratt School of Engineering, Duke University, Durham, North Carolina, USA | [3]Hunan Key Laboratory for Conservation and Utilization of Biological Resources in the Nanyue Mountainous Region, Hengyang Normal University, Hengyang, China | [4]Bordeaux Sciences Agro, INRA UMR 1391 ISPA, Gradignan, France | [5]Southern Research Station, USDA Forest Service, Research Triangle Park, Durham, North Carolina, USA | [6]CAS Key Laboratory of Tropical Forest Ecology, Xishuangbanna Tropical Botanical Garden, Chinese Academy of Sciences, Mengla, China | [7]University of Chinese Academy of Sciences, Beijing, China | [8]Yunnan Key Laboratory of Forest Ecosystem Stability and Global Change, Xishuangbanna Tropical Botanical Garden, Chinese Academy of Sciences, Mengla, China | [9]Department of Forest Sciences, University of Helsinki, Helsinki, Finland

**Correspondence:** Na Wang (wangnsilv@163.com) | Jean-Christophe Domec (jc.domec@agro-bordeaux.fr; jc.domec@duke.edu)

**Received:** 12 January 2025 | **Revised:** 4 June 2025 | **Accepted:** 6 June 2025

**Funding:** Na Wang gratefully acknowledges the financial support from the Scientific Research Project of Hunan Provincial Education Department (No.21B0642), and the Natural Science Foundation of Hunan Province (No. 2022JJ40012), and the Open Fund Project of Hunan Key Laboratory for Conservation and Utilization of Biological Resources in the Nanyue Mountainous Region (No.2021HSKFJJ036). Financial support for Ram Oren was provided by the Erkko Visiting Professor Programme of the Jane and Aatos Erkko 375th Anniversary Fund; additional support for Sari Palmroth and Ram Oren was provided by the ACCC Flagship – University of Helsinki, funded by the Academy of Finland (grant number 337549), both through the University of Helsinki. Some support was available from the Department of Energy, USA (No. DE-SC0023309), the Department of Defense, USA (SERDP RC-25-0189) and from the French ANR (grant PHYDRAUCC 21-CE02-0033-02) and the Nlle Aquitaine Region (Project VITIPIN AAPR2020-2020-8596610, GRIFFON and IMPACTS).

**Keywords:** bordered-pits | cell-wall thickness | conductance | conductivity | needle length | *Pinus* | resistance partitioning | xylem anatomy

## ABSTRACT

Plant hydraulics govern water transport linking root to mesophyll surfaces, affecting gas-exchange, survival and growth. Xylem and leaf structural and functional characteristics vary widely among *Pinus* species, even when growing under similar conditions. We quantified the variation of xylem anatomy, hydraulic function, and within-tree hydraulic resistivity distribution, among five widely ranging southern US species: *Pinus echinata*, *Pinus elliottii*, *Pinus palustris*, *Pinus taeda* and *Pinus virginiana*. We found that, across species, needle length (NL) explained most of the variation in needle hydraulic properties. Resistivity to water flow in needles through tracheids' bordered-pits decreased linearly from ~99% to 8% with increasing NL; total tracheid resistivity in branches and roots was partitioned between bordered-pits and lumens similarly regardless of NL. Mean annual precipitation typical of the species' climatic range (CR) accounted for the variation in root hydraulic properties. Despite strong root-to-branch correlations of several attributes, neither NL nor CR explained the variation of any branch attribute. The results suggest that NL dominates needle xylem anatomy and function in a manner consistent with increasing hydraulic efficiency with NL, but CR produces genetic differences resulting in increased resistance to more negative xylem pressures with decreasing precipitation, at a cost of reduced hydraulic efficiency.

https://doi.org/10.1111/pce.70015

## 1 | Introduction

Conifer trees are among the tallest organisms, and limitations imposed by the hydraulic pathway are thought to be the major constraint on their long-distance water transport capacity and their maximum attainable heights (Koch et al. 2004; Domec et al. 2008). Trees have evolved as hydraulically complex organisms (Tyree and Ewers 1991), and within-tree variation in xylem anatomy and hydraulic properties may occur because different organs fulfil different mechanical and hydraulic roles (Dunham et al. 2006; Schuldt et al. 2013). For example, water transport in roots occurs in a relatively stable environment, while leaves and branches are exposed to mechanical forces generated by additional factors (wind, rain and snow; Pittermann et al. 2006). Strong selection for mechanical stability can result in smaller conduit and denser wood, that incidentally increase branch hydraulic safety, even if such safety is not needed. This leads to an overbuilt system, structurally or hydraulically more conservative than necessary, often at the expense of efficiency. Several hypotheses predict how xylem structure should change along the root-to-leaf water transport pathway, optimising whole tree hydraulic efficiency (McCulloh and Sperry 2005; Creek et al. 2018). In stems, it has been amply demonstrated that the diameter of xylem conduits is wide at the stem base progressively narrowing towards the apex (Anfodillo et al. 2013; Rosas et al. 2019; Soriano et al. 2020). Although leaves have also been investigated as part of the hydraulic pathway, here too selection apparently favours conductive systems with traits minimising increase in resistance with increasing path length (Gleason et al. 2018; Petit et al. 2014; Lechthaler et al. 2019).

The hydraulic efficiency of different organs along the root-to-leaf flow path can be captured by hydraulic conductance ($K$) or area-specific hydraulic conductivity ($K_s$), and its inverse the hydraulic resistance ($R$) or area-specific hydraulic resistivity ($R_s$) (Tyree and Ewers 1991). Leaves represent the terminal plant part of the soil–plant–atmosphere continuum, making up a significant portion of the whole plant hydraulic resistance (Cochard et al. 2004; Domec, Noormets, et al. 2009; Wang et al. 2019). Several studies have looked at the partitioning of hydraulic resistances within angiosperm leaves, and the current consensus is that, in leaves, xylem hydraulic resistance ($R_{\text{xylem}}$) is about as limiting as outside-xylem hydraulic resistance ($R_{\text{outside-xylem}}$) (Sack et al. 2004; Nardini et al. 2005). In contrast to angiosperm leaves, a large variability exists among pine species in the fraction of total needle resistance located in the xylem, with values ranging from 24% in *Pinus mugo* (Charra-Vaskou and Mayr 2011) to 49% in *Pinus taeda* (Domec et al. 2016). In term of hydraulic permeability, recent results from a study on five pine species ranging in needle length (NL) from 7 to 36 cm (Wang et al. 2019) showed that across species, leaf, xylem and outside-xylem hydraulic conductance ($K_{\text{leaf}}$, $K_{\text{xylem}}$ and $K_{\text{outside-xylem}}$, respectively) scaled positively with NL. The increased hydraulic efficiency with NL was the outcome of increased xylem area and lumen diameter, and decreased mesophyll cross-sectional area and the ratio of mesophyll cell surface area to needle surface area. NL is therefore an important morphological trait, affecting hydraulic anatomy and function, water transport, and the partitioning of resistances between the xylem and outside-xylem components.

Moving through xylem, water encounters two principal resistances: the resistance along the lumen, and that imposed by end-wall pits (Becker et al. 2003). In roots, trunk-wood or branches, several studies reported that lumen- and pit-area scale isometrically, thus pit resistance represents a large fraction (55%–75%) of the whole tracheid resistance independently of conduit size or even species (Sperry et al. 2006; Domec et al. 2016; Schulte et al. 2015; Lazzarin et al. 2016). However, in leaves the effect of organ-specific trait differences on the distribution of xylem hydraulic resistance or resistivity between lumen and end-wall pits across species remains largely unquantified (Domec et al. 2016). Differences in hydraulic structure among organs, especially in leaves, and how hydraulic resistivity is partitioned, may reflect genetically induced patterns that consistently rank these traits across species. Because xylem conduits are arranged in series, it is reasonable to hypothesise that an increase in lumen axial water transport with NL could potentially increase the proportion of lumen resistance ($R_{\text{lumen}}$) to $R_{\text{xylem}}$ (i.e., $R_{\text{lumen}}/R_{\text{xylem}}$), or the proportion of area-specific lumen resistivity ($R_{\text{s-lumen}}$) to area-specific xylem resistivity ($R_{\text{s-xylem}}$) (i.e., $R_{\text{s-lumen}}/R_{\text{s-xylem}}$). In other words, we can expect that the proportion of area-specific end-wall pit resistivity ($R_{\text{s-pit}}$) should decrease with leaf size or path length (Zwieniecki 2004). However, differences among species in hydraulic properties may only exist in needles and be related to NL, because at this endpoint of transpiration, xylem structure-function is mostly driven by the demand to supply enough water to keep stomata open along the entire needle surface (Delucia et al. 2000). Elsewhere along the whole-plant hydraulic pathway, xylem traits may be more sensitive to environmental pressures, reflecting both the conditions of the species' range and where the sampled individuals grow (Kilgore et al. 2021).

Many studies aimed to understand the links between functional traits and species distribution (Li et al. 2018; Liu et al. 2021). Although species distributions along environmental gradients have generally been well documented, the mechanisms driving the distributions are less well known (Pfautsch et al. 2018; He et al. 2020). In conifers, vulnerability to drought-induced embolism increased from low in species from semiarid zones to high in species from wet environments (Brodribb et al. 2014). Given the strong selective force exerted by water stress on vegetation, the distribution of pine species along environmental gradients can indeed be expected to be influenced by their embolism resistance (Pockman and Sperry 2000; McCulloh et al. 2019). Pine roots tend to exhibit relatively high vulnerability to xylem embolism (Zhang et al. 2025); nevertheless, many species such as ponderosa pine (*Pinus ponderosa*) and piñon pine (*Pinus monophylla*) are well adapted to persist in arid environments (Maherali and DeLucia 2000; Johnson et al. 2016). Hacke et al. (2001) demonstrated that embolized conduits experience large bending stresses that could lead to cell collapse under large negative xylem pressures. The basis for this relationship is that the double-cell wall shared by adjacent cells behaves in a manner similar to a long plate of width $b$ (cell diameter) and thickness $t$ (double-cell wall thickness), a plate that will buckle under a force proportional to $(t/b)^2$. Several studies demonstrated that species distribution and adaptation to arid and mesic environments correspond to variations in tracheid structure and their effect on hydraulic traits (Sperry et al. 2006; Pritzkow et al. 2020). Xylem anatomy determines the hydraulic conductance of a particular plant organ (Hacke et al. 2001; Bouche et al. 2014), providing the structural basis for species-dependent differences in $K_{\text{xylem}}$, $K_{\text{s-xylem}}$ and $(t/b)^2$.

Quantifying plant structural and functional traits in relation to the distribution of species along environmental gradients is therefore essential to advancing understanding of current and projections of future distribution patterns of pine and other species (Augustine and McCulloh 2024). However, hydraulic traits within and among species reflect not only the genetic differences imposed by morphological differences (e.g., NL) and environmental conditions of the species' native climatic range (CR), but also the conditions where sampled individuals are growing. Common garden studies can help isolate the genetically induced effects from effects imposed by the growing conditions (Jankowski et al. 2019; Duboscq-Carra et al. 2020). If needle morphological differences are not strongly related to the environmental conditions in the original range, attribution of the variation of hydraulic traits can be allocated to either of the genetically induced sources (NL or CR).

We studied five pine species from a broad climatic gradient within the southeastern United States, *Pinus echinata*, *Pinus elliottii*, *Pinus palustris*, *P. taeda* (two families), *Pinus virginiana* in a common environment. All five species are shade intolerant, relatively well-adapted to poor soils, and show overlapping geographical ranges, each with at least two others. We assess the trait values of these co-occurring, related species as independent solutions of functional hydraulic systems. Our goal was to gain a more in-depth understanding of within-organism variations and linkages in hydraulic resistivity distribution, and hydraulic anatomical and functional traits in these pines. We further explored whether these variations, in different organs across species, were better explained by NL or by CR, the climate of origin in the distributional range of these species. While recent previous work established correlations between NL and their anatomical and gas-exchange properties (Wang et al. 2019), our study takes a broader perspective by assessing whether NL or CR more strongly influences trait variation across multiple organs and species.

Specifically, we hypothesised that: **(H1)** Branch-root correlations of a given trait will be stronger than either leaf-branch or leaf-root. This is because the first two are involved in only longitudinal transport, while needle structure and function must accommodate radial transport as well. Because needle xylem traits are likely to have poorer correlations with those of branches and roots, and based on earlier analyses (Wang et al. 2019), we hypothesised that **(H2)** needle xylem traits will be best explained by NL. Finally, because hydraulic performance of branch and root xylem has been shown to be affected by environmental conditions (Ewers et al. 2000; Maurel and Nacry 2020), we hypothesised that **(H3)** xylem traits of roots and branches will be best explained by CR, reflecting minimum temperature and aridity (Bouche et al. 2014). Alternatively (to **H3**), these xylem attributes may not vary much among species, reflecting acclimation to the common environment in which individuals of all five species are growing.

## 2 | Materials and Methods

### 2.1 | Site Description

In 2011, 1-year-old seedlings of *P. echinata* Mill., *P. elliottii* Engelm., *P. palustris* Mill., *P. taeda* L. (two families), *P. virginiana* Mill. were planted in 32 × 40 m plots (4 × 2 m spacing), at a site characterised by sandy loam soil of the Appling series, in the Duke Forest, Durham, NC, USA (36°01′ N, 78°59′ W). The climate of the region is warm and humid with a mean annual temperature (MAP) of 15.5°C, and annual precipitation of 1145 mm (average between 1992 and 2021) distributed evenly throughout the year. *P. echinata* and *P. elliottii* seedlings issued from a second generation progeny test came from Flint River Nursery, Byromville, GA. *P. palustris* plot was planted with seedlings of various provenances across the southeastern USA (Longleaf Pine Regional Provenance/Progeny Trial, NC State University Cooperative Tree Improvement Program and USDA Forest Service, Raleigh, NC). *P. taeda* seedlings were from Supertree Nursery, Blenheim SC, and contained two mass-control pollinated families (ArborGen Inc., Ridgeville, SC), with broad (AGM-37) and narrow (AGM-22) crown characteristics. *P. virginiana* seedlings were from Claridge Nursery, Goldsboro, NC. At the end of the 2017 growing season, the dominant heights of *P. echinata*, *P. elliottii*, *P. taeda* and *P. virginiana* were 3.3, 4.4, 6.6 and 3.9 m, respectively. *P. palustris* trees showed a large range of heights due to the distinctive developmental pattern of the species (averaging 1.4 m in our plot), but sampled individuals passed the 'bottlebrush' stage and were ~2 m tall in the fall of 2017 (Wang 2021).

### 2.2 | Hydraulic Measurements

Hydraulic measurements were conducted on 3–4-year-old branches and current-year needles harvested in October 2015, and 3–5-year-old roots dug in July 2017. Climate was quite similar in the different sampling years, with precipitation ranging 1200–1385 mm per year, above the 30-year average. Branches, 3.7–12.4 mm in diameter, were collected from the upper section of tree crowns, and coarse roots, 5.3–13.8 mm, from 10 to 20 cm soil depth, from five randomly sampled individuals per species. Root excavations down to 100 cm, performed in the middle of each plot in June 2020, revealed that more than 60% of the roots of all species were located within the upper 20 cm of soil and > 75% within the upper 40 cm. To prevent extraneous surface resistance by resin leaking from broken resin canals, before the first hydraulic measurements, we removed excess resin by soaking the cut surfaces in water for 60–90 min, and then recut the end-surfaces with a clean razor blade (Booker 1977; Bonetti et al. 2021). In this study, we use both conductance (or conductivity) and resistance (resistivity) depending on the expression most useful for explaining the controls on the hydraulic function across the five species (Melcher et al. 2012). Because resistances add in series, the measured values for branches can be partitioned into their resistance components (stem and leaves).

Hydraulic conductivities were determined using a hydraulic conductance flow metre (HCFM, Tyree et al. 1995; Zotz et al. 1998) using the formula: $K = Q_v/\Delta P$; where $Q_v$ is the volumetric flow rate ($\text{kg s}^{-1}$) and $\Delta P$ is the applied pressure gradient (MPa) across a sample. This technique was used because it is rapid, allowing to determine the hydraulic conductance of the whole organs and partition the contribution of conductivity between xylary and outside-xylem water pathways (Tsuda and Tyree 2000). The cut ends of branches were connected to the HCFM (Dynamax Gen2, IN, USA) using a watertight seal, and deionized and degassed water filtered at 0.1 µm was delivered at a pressure of 0.2–0.3 MPa. Note that preliminary tests indicated that $K$ values determined at pressures ranging from 0.01 to 0.45 MPa were statistically similar (slope = 0.06, $R = 0.04$; $p = 0.88$). During HCFM measurements, the leaves were submerged in water to maintain constant temperature and prevent transpiration. Hydraulic conductance was standardised to values for 25°C to account for the effects of temperature on water viscosity. Whole branch hydraulic conductance ($K_{\text{branch}}$; kg $\text{MPa}^{-1}\,\text{s}^{-1}$) was recorded every 30 s and shown to increase during the first 3–5 min. Data points were recorded after stable values were reached corresponding to a coefficient of variation < 5% for the last 10 readings. After $K_{\text{branch}}$ ($1/R_{\text{branch}}$) was obtained, needles were immediately removed at their connections to the woody stem using a new blade, and the hydraulic conductance reassessed ($K_{\text{stem}} = 1/R_{\text{stem}}$). Measurements took 8–12 min for an intact shoot, and an additional 5–10 min after needle removal. $R_{\text{leaf}}$ ($=1/K_{\text{leaf}}$) was calculated by subtracting $R_{\text{stem}}$ from $R_{\text{branch}}$ (Luo et al. 2023).

On another set of branches, $K_{\text{branch}}$ and $K_{\text{leaf}}$ were obtained from frozen-thawed needles (frozen 10 min at −55°C, thawed at +23°C for 30 min). Freezing needles disrupts cell membranes and removes the hydraulic resistance of the outside-xylem water pathway (Cochard et al. 2004; Nardini et al. 2005; Domec et al. 2016). Therefore, we used $K_{\text{leaf}}$ estimated from frozen needles to represent the conductance of the needle xylem located in the central vein (leaf $K_{\text{xylem}}$). Preliminary tests on six shoots showed that $K_{\text{branch}}$, once stable, remained so for 15 min, the period during which removing needles and re-measuring were completed. We note that, in our measurements, the freeze-thaw process should not cause embolism, since thawing did not occur under tension (Pittermann and Sperry 2006). All leaf hydraulic resistance and conductance variables were normalised by projected branch needle area (giving $R_{\text{leaf}}$ in $\text{m}^2\,\text{s}\,\text{MPa}\,\text{kg}^{-1}$ and $K_{\text{leaf}}$ in $\text{kg}\,\text{m}^{-2}\,\text{s}^{-1}\,\text{MPa}^{-1}$) estimated by analysing images of scanned needles with Image-J (National Institutes of Health, MD, USA). The xylem hydraulic specific conductivity ($K_{\text{s-xylem}}$) in needles was calculated as: leaf $K_{\text{xylem}} \times$ needle projected area × NL/needle xylem area ($\text{kg}\,\text{m}^{-1}\,\text{s}^{-1}\,\text{MPa}^{-1}$).

Specific hydraulic conductivity of the xylem ($K_{\text{s-xylem}}$) of branch stems and root segments was also measured with the HCFM and was calculated as: $Q_v \times L/(A_s \times \Delta P)$, where $L$ and $A_s$ are the length and the cross-sectional area of the measured sample. Leaf specific conductivity (LSC) was calculated as: branch $K_{\text{s-xylem}} \times A_s$/needle projected area.

## 2.3 | Leaf, Branch and Root Anatomy and Computed Hydraulically Related Variables

Additional fresh needles, branches and roots were collected in 2017 from five random trees per species for anatomical measurements. Anatomical features were determined from hand-made sections (~40 µm thickness) cut in the middle region of the samples using razor blades. The cross-sections were photographed at ×400, ×100 and ×100 magnification for needles, branches and roots, respectively, using a digital camera mounted on a compound microscope (iScope trinocular IS1153-PLi, AmScope, USA). Two, eight-to-ten and four-to-six images were taken per cross-section for needles (from five needles per tree), branches, and roots (one sample per tree), respectively, together covering most of the xylem area of the cross-section from each sample. The images were analysed using the Motic Images Advanced 3.2 software (Motic Corporation, Zhejiang, China).

We computed hydraulically related variables from tracheid anatomical features. Tracheid lumen diameter ($b$), tracheid double cell-wall thickness ($t$), the number of tracheids ($N$), and total tracheid area ($A$) of all individual conduits from each cross-sectional image were measured. Total tracheid diameter ($d_t$) was calculated as the sum of $b$ and $t$; tracheid density ($D_t$ = number of conduits per $\text{mm}^2$) was calculated as N/A.

Mean tracheid hydraulic diameter ($d_h$) was calculated as $d_h = (1/n \sum_{i=1}^{n} \text{b}_\text{i}^{4})^{1/4}$ where $b$ is the $i$th tracheid lumen diameter and $n$ is the total number of tracheids (Tyree and Zimmermann 2002). Hydraulic conductance of coniferous tracheids is a function of both the tracheid lumen conductance and bordered-pit conductance connected in series. According to the Hagen–Poiseuille law (Tyree and Ewers 1991), the lumen (axial) specific hydraulic conductivity $K_{\text{s-lumen}}$ ($\text{kg}\,\text{m}^{-1}\,\text{s}^{-1}\,\text{MPa}^{-1}$) was calculated as $K_{\text{s-lumen}} = (\pi\rho/128\eta A) \sum_{i=1}^{n} \text{b}_\text{i}^{4}$, where $A$ is sampling area, $\rho$ is the density of water and $\eta$ is the viscosity of water at 25°C. The bordered-pits hydraulic specific hydraulic conductivity ($K_{\text{s-pit}}$) was calculated as $K_{\text{s-pit}} = 1/(1/K_{\text{s-xylem}} - 1/K_{\text{s-lumen}})$ (Domec et al. 2006).

The calculation of hydraulic diameter in leaves was more complicated than that in branches and roots. The assumption of equal-sized tracheids and equal tracheid density holds for much of the needle but diverges to some degree at the very tip and so using anatomical values measured in the centre of a needle as a proxy for the whole needle average may produce a bias. We therefore corrected our centred values by a factor of 0.96 to account for the slight decline in tracheid size with NL (Zwieniecki et al. 2006; Domec et al. 2016), which allowed estimation of the integrated $K_{\text{s-lumen}}$ based on the size and number of tracheids measured in the middle section of the needles.

## 2.4 | Species Geographic Distribution and Climatic Factors

The geographic distribution of each pine species was obtained from the Gymnosperm Database (http://www.conifers.org/index.php). For each pine species, 20 sites were selected at the distribution boundary and the average climate of those sites were calculated to represent the climate condition of the entire distributional range (CR). The climatic factors, mean annual precipitation (MAP) and MAT, and the number of days temperature dropped below 0°C of each site were collected from National Oceanic and Atmospheric Administration (US) https://www.climate.gov/. Aridity data were collected from CGIAR-CSI Global Aridity Index (Global-Aridity) and Global

Potential Evapo-Transpiration (Global-PET) Climate Database (Trabucco and Zomer 2009).

### 2.5 | Data Analysis

Anatomical traits measured or calculated from needle, branch and root samples were averaged for individual trees, then, the means and standard errors ($n = 5$) of all the anatomical traits and hydraulic-related variables for each species were calculated. The definition of variables is shown in Table 1.

To assess the consistency of hydraulic traits among organs, we correlated each anatomical and functional variable among needles, branches and roots, and tested how anatomical variables affected hydraulic performance. The relationships between anatomical and hydraulic traits were assessed using Pearson correlation coefficients and principal component analysis (PCA). Mean values for each species from the two main PCA axes were examined for organ-specific relationship with NL, MAP and MAT. The dimension reduction offered by PCA helps identify patterns in the data, however, while it retains much of the information in the original variables it allows only broad interpretation. We thus followed the PCA analyses quantifying (1) how well the variables reflecting CR affected NL, and (2) how well NL and CR explained the variation in specific hydraulic anatomical and functional traits, adding detail to the results from the lumped PCA axis values. The variables used in this last set of analyses represent the ability of the xylem to resist cell-wall collapse, $(t/b)^2$, the hydraulic diameter ($d_h$), and the three hydraulic conductivity variables, which are either directly measured or computed.

Pearson's correlation and PCA analyses were performed in R version 3.6.3 (R Core Team 2019), and curve fits using SigmaPlot (version 12.5, Systat Software Inc., San Rafael, CA, USA).

## 3 | Results

### 3.1 | Correlations Among Hydraulic Variables Within Organs

Of the anatomical, and anatomically-based variables, the among-species range of diameter-related properties [tracheid diameter [$d_t$], lumen diameter [$b$] and hydraulic diameter [$d_h$]) and cell-wall thickness ($t$) was smallest in needles and largest in roots, while tracheid density ($D_t$) showed an opposite trend (Supporting Information S1: Table S1). The range of thickness-to-span ratio ($[t/b]^2$) among species was highest in branch, and smallest in root (except *P. virginiana* and *P. echinata*) (Supporting Information S1: Table S1). The three diameter-related variables, $d_t$, $b$ and $d_h$, were highly positively correlated, and strongly inversely correlated with $D_t$ across species in all organs (Figure 1a–c). Because cell wall thickness (*a* component of $d_t$) is small relative to $b$ (Supporting Information S1: Table S1), and because $d_h$ is computed from b, both measured variables were also highly correlated to $d_h$. Furthermore, because the higher $d_t$ is, the fewer tracheids fit per unit of area, all three variables were strongly inversely correlated with $D_t$. However, although the three diameter-related properties ($d_t$, $b$, $d_h$) were positively correlated with $t$ in leaves (strongly) and branches (close to significant), in roots they were uncorrelated with $t$ (Figure 1c). In contrast, the resistance to cell-wall implosion under negative xylem pressures in branches and roots, reflected in $(t/b)^2$, was strongly negatively associated with diameter-related properties, thus positively related to $D_t$, but these correlations were not found in the leaves (Figure 1a).

Among the functional variables, across species, leaf and branch specific hydraulic conductivity of the lumen ($K_{s\text{-lumen}}$), computed from anatomical variables (Table 1), was positively correlated with the specific xylem hydraulic conductivity ($K_{s\text{-xylem}}$). In contrast, the specific hydraulic conductivity of pits ($K_{s\text{-pit}}$) was strongly correlated to $K_{\text{s-xylem}}$ in all organs, showing the dominance of pits in the hydraulic function of the xylem.

### 3.2 | Correlations of Xylem Anatomical and Functional Traits Among Organs

None of the anatomical variables were significantly correlated between leaf and branch (Figure 1d). Interestingly, the $t$ variable was the only one showing correlation between leaf and root (Figure 1e). Two diameter-related properties ($d_t$, $b$) and $D_t$ were positively correlated between branches and roots, while $t$ was not correlated (Figure 1f), perhaps owing to its small variation in branches among species (3%; Supporting Information S1: Table S2). Finally, stronger branch-root (than either leaf-branch or leaf-root) correlations observed in diameter-related properties ($d_t$, $b$) and $D_t$ were also observed in the functional variables, reflecting the contribution of the anatomical variables.

**TABLE 1** | Variables describing anatomical and functional hydraulic properties.

| Measured variables | Computed variables | Contributing variables |
|---|---|---|
| Anatomy | | |
| Lumen diameter ($b$) | Tracheid diameter ($d_t$) | $b$, $t$ |
| Tracheid density ($D_t$) | Hydraulic diameter ($d_h$) | $b$ |
| Tracheid cell-wall thickness ($t$) | (Tracheid cell-wall thickness/lumen diameter)$^2$ $(t/b)^2$ | $t$, $b$ |
| Function | | |
| Specific xylem conductivity ($K_{\text{s-xylem}}$) | Specific lumen conductivity ($K_{\text{s-lumen}}$) | $d_h$, $D_t$ |
| | Specific pit conductivity ($K_{\text{s-pit}}$) | $K_{\text{s-xylem}}$, $K_{\text{s-lumen}}$ |

*Note:* Four measured variables were used to compute five additional variables.

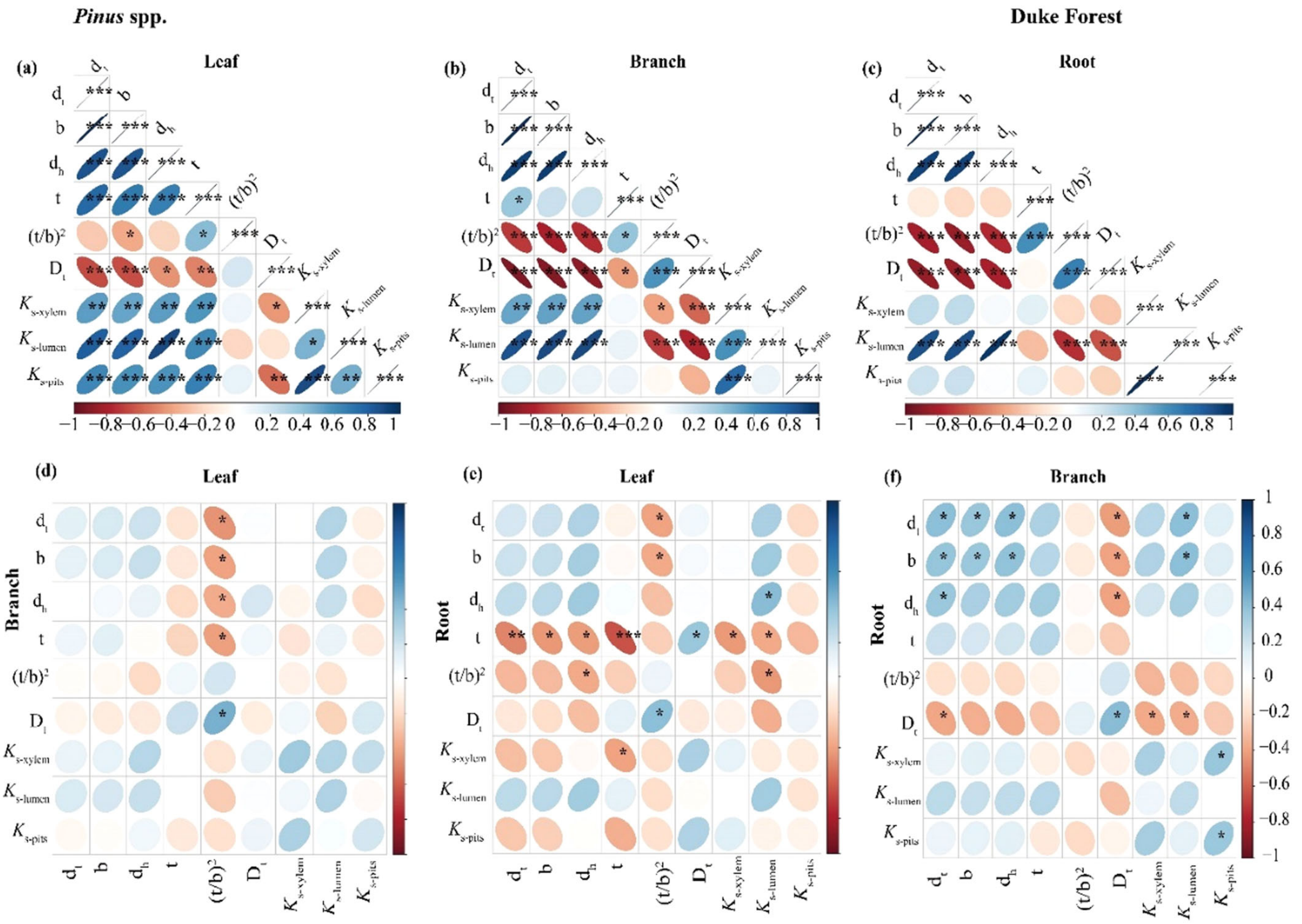

**FIGURE 1** | Pearson's correlations among anatomical and functional properties within leaf (a), branch (b) and root (c), as well as the comparison across species between (d) leaf versus branch, (e) leaf versus root, and (f) branch versus root. *, $0.01 < p < 0.05$; **, $0.001 < p < 0.01$; ***, $p < 0.001$. Colour and orientation of the ellipses depend on the strength and the sign of the correlation (the intensity of colour increases uniformly as the correlation value moves away from 0 with blue for positive values and red for negative ones). In addition, the ellipses have their eccentricity parametrically scaled to the Pearson's correlation values. [Color figure can be viewed at wileyonlinelibrary.com]

## 3.3 | The Dependence of Hydraulic Function on Hydraulic Anatomy

The three diameter-related variables ($d_t$, $b$, $d_h$) explained much of the variation among species in $K_{\text{s-lumen}}$ in all three organs (Figure 1a–c), reflecting strong correlations between these anatomical parameters, and the fact that $d_h$ is used in calculating $K_{\text{s-lumen}}$. These three variables were also important in explaining the variation of $K_{\text{s-xylem}}$ and $K_{\text{s-pits}}$ in leaves and $K_{\text{s-xylem}}$ in branches, but not in roots, consistent with the correlations between $K_{\text{s-xylem}}$ and $K_{\text{s-lumen}}$ or $K_{\text{s-pit}}$ (Figure 1c). We note that, among these relationships, the only ones with no autocorrelation are those involving $K_{\text{s-xylem}}$ and any anatomically-based variables. The positive relationships between $d_t$, $b$ and $d_h$ and $K_{\text{s-xylem}}$ were strongest in leaves and weakest in roots, and perhaps the negative one between $K_{\text{s-xylem}}$ and $(t/b)^2$ in branches deserve most attention.

Other strong positive and negative relationships are driven by the correlation strength and direction among anatomically-based variables, and the degree of autocorrelation which depends on whether one or more variables were used in the calculation of the dependent variables. As examples: (1) $D_t$ showed inverse patterns with specific conductivities ($K_{\text{s-xylem}}$, $K_{\text{s-lumen}}$, $K_{\text{s-pits}}$) in all organs (Figure 1a–c), which is a reflection of the strong negative correlation between $D_t$ and diameter-related properties ($d_t$, $b$, $d_h$); (2) $(t/b)^2$ was strongly negatively correlated with $K_{\text{s-lumen}}$ in branches and roots, but not in leaf, consistent with the correlations between $d_t$, $b$, $d_h$ and $(t/b)^2$.

## 3.4 | Distribution of Species Relative to Their Leaf, Branch and Root Anatomical and Functional Traits

Together, the first two axes of the PCA explained 79%, 78% and 72% of the variability in leaf, branch and roots, respectively (Figure 2). The first axis, representing the anatomical variables and accounting for ~60% of the variance, showed that tracheid diameter-related properties were dominant and opposite to tracheid density. On the second axis, $(t/b)^2$ was particularly dominant in leaves (Figure 2a), whereas $t$ and $K_{\text{s-pits}}$ were positively correlated in branches and roots (Figure 2b,c). In addition, PCA separated some of the species based on differences between organs. In leaves, *P. virginiana*

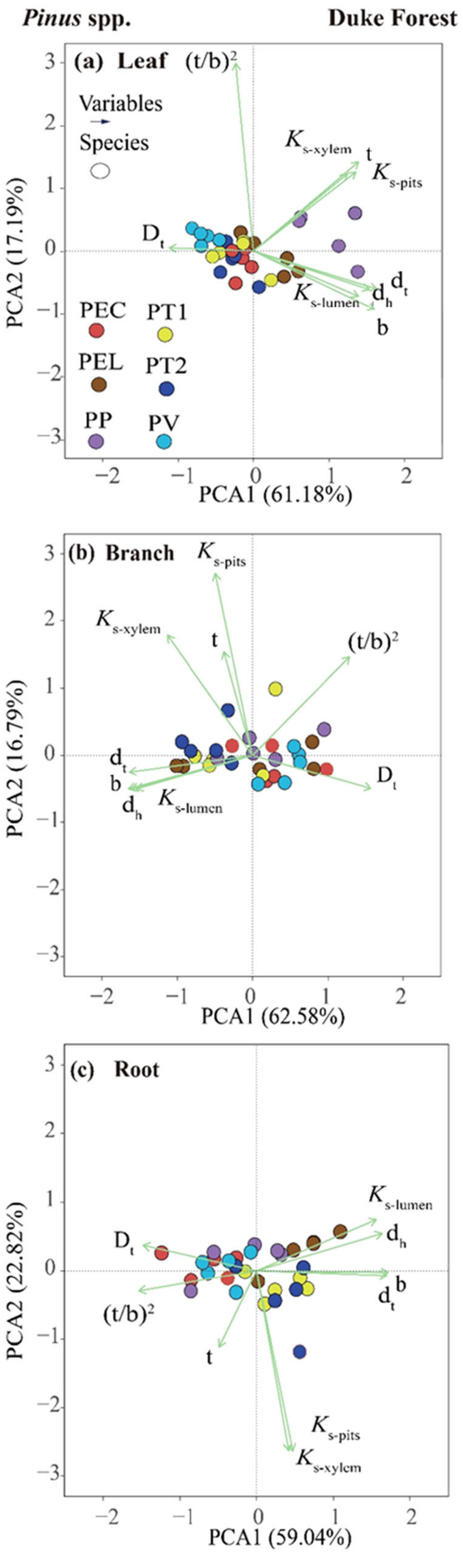

**FIGURE 2** | Principal component analysis (PCA) of leaf traits (a), branch traits (b) and root traits (c). The first PCA axis represents the hydraulic efficiency dimension, with larger diameter-related variables (tracheid diameter [$d_t$], lumen diameter [b], hydraulic diameter [$d_h$] and tracheid lumen conductivity [$K_{\text{s-lumen}}$]) placed opposite to low tracheid density ($D_t$) in all organs, and to cell thickness-to-span ratio [$(t/b)^2$] in roots. PV, *Pinus virginiana*; PEC, *Pinus echinata*; PT1 and PT2, *Pinus taeda*; PEL, *Pinus elliottii*; PP, *Pinus palustris*. [Color figure can be viewed at wileyonlinelibrary.com]

and *P. echinata*, species bearing short needles, were distinguished from long-needle species, that is, *P. palustris* and to some extent *P. elliottii*. In branches, *P. virginiana* and *P. echinata* were distinguished from *P. taeda* and in roots also from *P. elliottii*.

Variation among species means in the first PCA axis values were mostly explainable by NL in leaf and by MAP and to some extent by MAT of the species' natural range in roots (Figure 3). Neither NL nor MAP or MAT explained the variation along the second PCA axis values (Supporting Information S1: Figure S1).

### 3.5 | Effect of NL on Xylem Anatomical and Hydraulic Variables

A complete presentation of the amount of variation in each measured and computed variable explained by NL and CR is given in Supporting Information S1: Table S3. Regardless of whether *P. palustris* was included or not, the ability of leaf xylem to resist collapse under negative pressure (represented by $[t/b]^2$) was unrelated to NL (Figure 4a), but most of the across-species variation in leaf $d_h$ and all three forms of leaf conductivity (pit, lumen and xylem) was explained by NL (Figure 4b,c). In contrast, NL did not explain much of the variation among species in these variables in branches and roots (Supporting Information S1: Table S3). However, when *P. palustris* was again excluded from the analyses, NL explained most of the variance in $(t/b)^2$ and $d_h$, and in its corollary $K_{\text{s-lumen}}$ in the roots of the five populations (Figure 4d–f).

While conductivities presented here are based on xylem area, we also calculated whole-branch leaf-specific conductivity (LSC). The results were principally similar or weaker because of the linear correlation between branch specific hydraulic conductivity of the xylem ($K_{\text{s-xylem}}$) and LSC ($R^2 = 0.52$, $p = 0.01$). However, unlike branch $K_{\text{s-xylem}}$ which was uncorrelated to NL (Supporting Information S1: Table S3), LSC was more strongly correlated with NL than branch $K_{\text{s-xylem}}$ ($R^2 = 0.76$, $p = 0.02$, Supporting Information S1: Figure S2).

Using the ohm (electrical resistance) analogy applied to a hydraulic circuit, the total resistivity to water flow in tracheids was partitioned between lumen and end-wall bordered pits. Among plant organs, leaves showed the largest among-species differences in the hydraulic resistivity partitioning between $R_{\text{s-lumen}}$ and $R_{\text{s-pit}}$. Across species, the mean ratio of pit resistivity to xylem resistivity ($R_{\text{s-pit}}/R_{\text{s-xylem}}$) increased progressively from 67% in leaves, to 69% in branches, and to 88% in roots (Figure 5). $R_{\text{s-pit}}/R_{\text{s-xylem}}$ was strongly correlated with NL in needles (Figure 5a), however, this relationship was weaker in branches and was not observed in roots (Figure 5b,c). None of the CR variables explained the variation in the proportion of resistivity to flow in any of the organs (Supporting Information S1: Table S4).

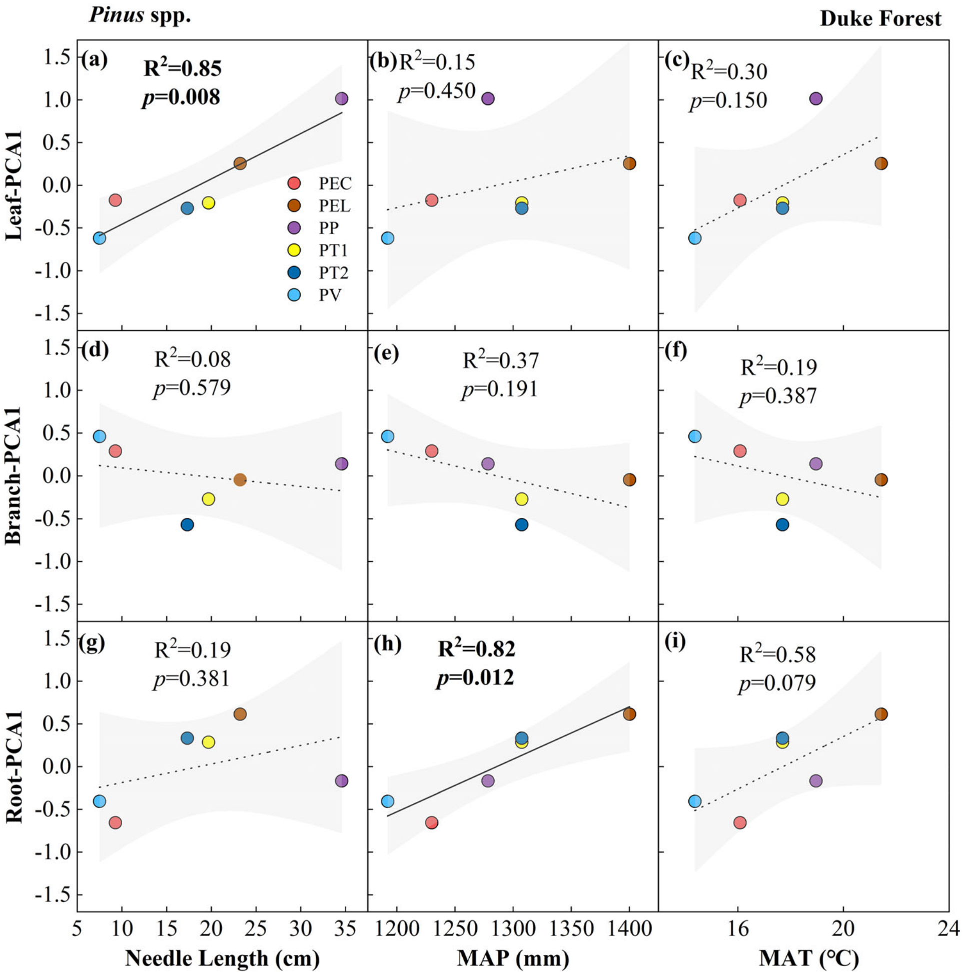

**FIGURE 3** | Variation in the scores of the first principal component axis (PCA1) of leaf traits (a–c), branch traits (d–f) and root traits (g–i) with needle length, mean annual precipitation (MAT) and temperature (MAT) of the species' natural range. PCA1 values are species means from Figure 2. PV, *Pinus virginiana*; PEC, *Pinus echinata*; PT1 and PT2, *P. taeda*; PEL, *Pinus elliottii*; PP, *Pinus palustris*. Dotted regression lines represent nonsignificant relationships ($p > 0.05$). [Color figure can be viewed at wileyonlinelibrary.com]

## 3.6 | Effect of Climate of Origin and Vpd on Xylem Structural and Hydraulic Variables

Across species, NL increased with MAT ($p = 0.09$; Supporting Information S1: Table S5), and decreased with the number of days of temperature $< 0°C$ ($p = 0.07$; Supporting Information S1: Table S5). MAP, growing season vapour pressure deficit (VPD), or aridity index did not explain the variation in NL. However, there was a clear departure of only *P. palustris* NL from potential relationship with MAP (Figure 6); excluding this species from the analyses resulted in MAP explaining more variation than the other variables, followed by MAT and the number of frost days (Figure 6, Supporting Information S1: Table S5). A correlation matrix among the variables representing the climate of the natural range of each species demonstrated that information captured in MAP represents both MAT and number of frost days well (Supporting Information S1: Table S6), meaning that additional variation in the hydraulic variables may be explained mostly by VPD and the aridity index.

Of the climate variables, none explained the variation among species in leaf hydraulic variable as well as did NL, regardless of whether *P. palustris* was included or not (Figure 7a–c, Supporting Information S1: Table S3). However, removing *P. palustris* from the analyses, increased the amount of the variation in leaf $d_h$ and the conductivity variables explained by MAP (Figure 7b,c). Moreover, of the CR variables, MAP explained most of the variation in $(t/b)^2$, $d_h$ and $K_{\text{s-lumen}}$ of roots (Supporting Information S1: Table S3; Figure 7d–f).

In branches, the only environmental variable correlated significantly with some of the hydraulic variables was VPD (Supporting Information S1: Table S3). Although VPD explained the variation in lumen and tracheid diameter, there was no correlation with cell wall thickness and consequently $(t/b)^2$ (Supporting Information S1: Table S3). Thus, only the variations in $K_{\text{s-lumen}}$ and, to a lesser degree, $K_{\text{s-pit}}$ were explained by VPD, and even these relationships were mostly driven by the lower values of *P. virginiana* (Supporting Information S1: Figire S3).

## 4 | Discussion

This study aimed to clarify the sources of within-organism variation in hydraulic resistivity and related anatomical and

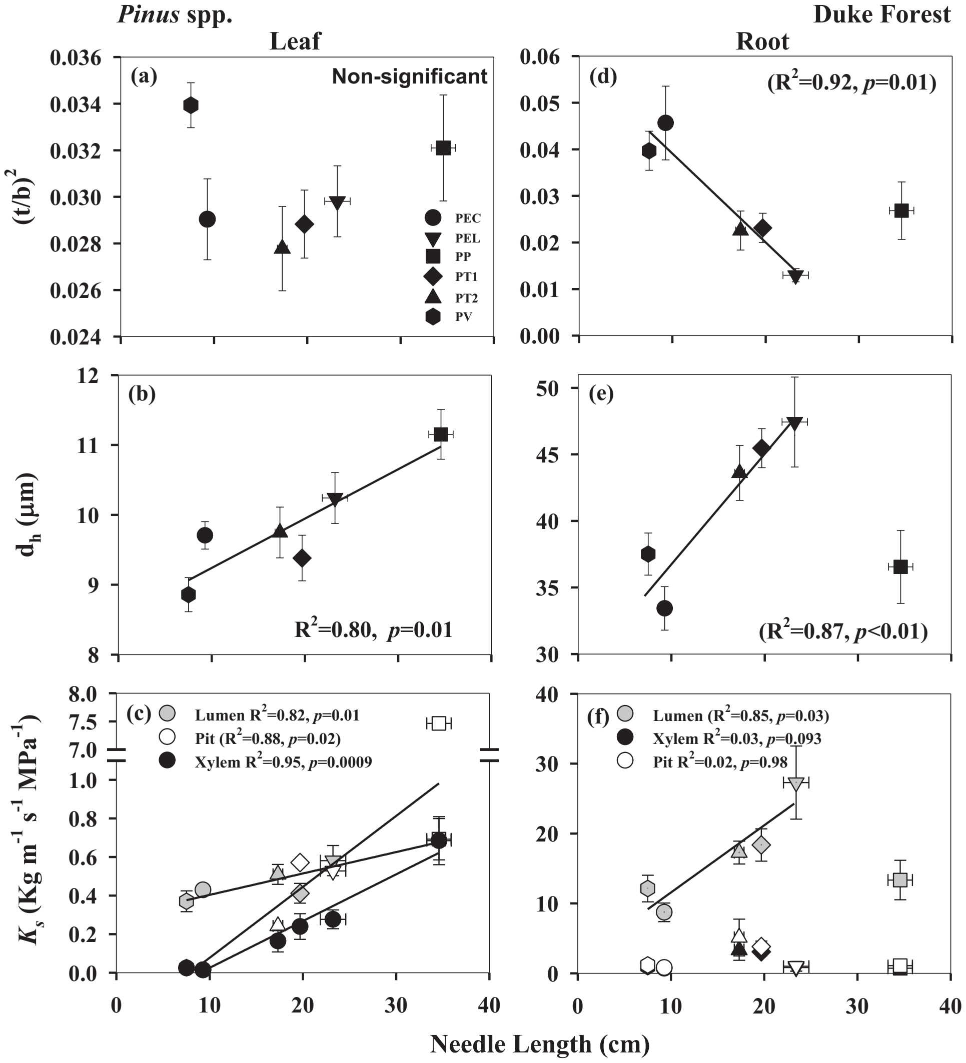

**FIGURE 4** | The response of anatomical and functional variables to increasing needle length in leaf (left panels) and root (right panels) of the five species studied. See Table 1 for definitions of variables. Note that roots have appreciably higher values for most variables. Note also that statistics are given in parenthesis when *Pinus palustris* is excluded from the regression analysis; for statistics inclusive of that species see Supporting Information S1: Table S3. PV, *Pinus virginiana*; PEC, *Pinus echinata*; PT1 and PT2, *Pinius taeda*; PEL, *Pinus elliottii*; PP, *P. palustris*.

functional traits across five widely distributed pine species. Performed at a common garden, thus isolating the genetic effects from environmental ones, we observed strong genetic control over anatomical variables and subsequently on hydraulic traits. The climate of origin (CR) was the driver of NL, and together, these variables significantly contributed to the variations in anatomical and functional traits of needles and roots (Figure 8).

## 4.1 | Correlations Among Hydraulic Variables Within and Among Organs

Branch-root correlations were stronger than either leaf-branch or leaf-root in hydraulic anatomical and functional traits (except for $t$; Figure 1d–f), supporting our **H1**. This could be caused by the fact that water transport in branches and roots occurs mainly in xylem. While in leaves, in addition to transport in the xylem, transfusion tissues and mesophyll characteristics may also have large effect on water transport.

Within and among species, PCA showed how anatomical and hydraulic traits are linked (Figure 2). The diameter-related variables (tracheid diameter [$d_t$], lumen diameter [$b$], hydraulic diameter [$d_h$]) were correlated with $K_{\text{s-lumen}}$ and strongly inversely correlated with tracheid density ($D_t$) across species and in all organs (Figures 1 and 2), which can be explained by cell 'packing limit', that is, that the space available for conduits is bounded by xylem cross-sectional area (McCulloh et al. 2010). Of hydraulic anatomical properties, tracheid cell-wall thickness ($t$) scaled positively with these three, tracheid diameter-related properties in leaves and branches (Figures 1a,b and 2a,b), indicating structural coordination within the aboveground xylem water transport system. In conifers, tracheids have a role both in water transport and in mechanical support. Previous studies have indicated that the thickness-to-span ratio ($[t/b]^2$) is important for the mechanical strength (Pittermann et al. 2006). The fact that cell-wall thickness and tracheid diameter-related properties varied in the same way may reflect the requirement of mechanical support in leaf and branch, whereas distal roots are supported by the soil and do not require strong mechanical support (Rosner et al. 2007).

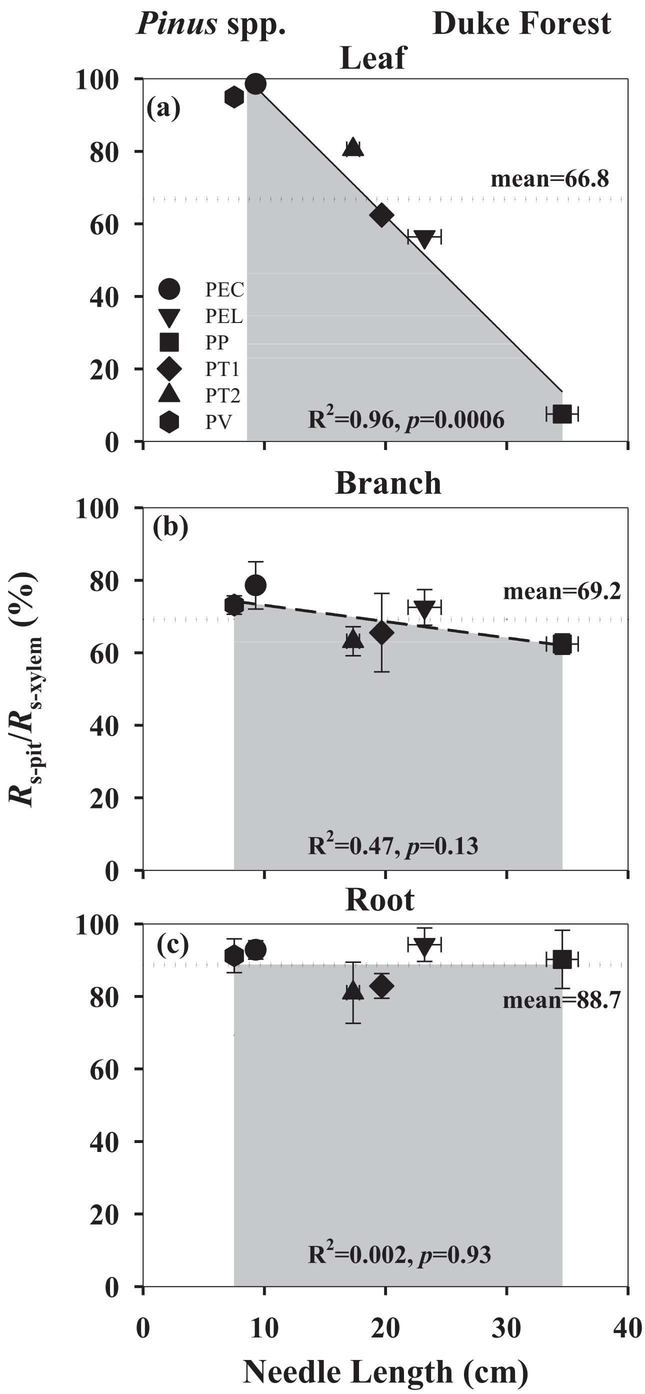

**FIGURE 5** | Change in the proportion of resistivity to water flow in xylem tracheids attributed to end-wall bordered pits ($R_{\text{s-pit}}/R_{\text{s-xylem}}$; reflected in the size of the grey area) in (a) leaves, (b) branches, and (c) roots as a function of increasing needle length. The areas above the regression lines represent the remaining proportion of hydraulic resistance located in the tracheid lumen. The dotted horizontal line is the percent mean across the six populations of the five species. PV, *Pinus virginiana*; PEC, *Pinus echinata*; PT1 and PT2, *Pinus taeda*; PEL, *Pinus elliottii*; PP, *Pinus palustris*.

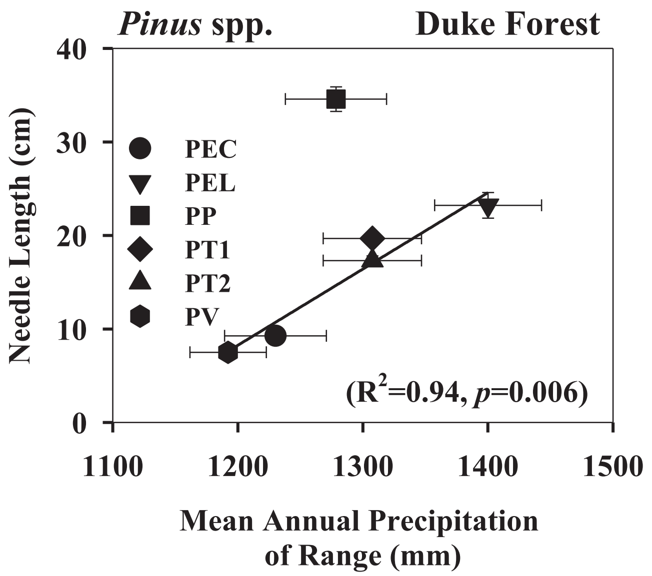

**FIGURE 6** | Needle length as a function of mean annual precipitation (MAP) of the species' natural range. The statistics are in parenthesis to emphasise that *Pinus palustris* is excluded from the regression analysis. Relationships including *P. palustris* are $R^2 = 0.30$, $p = 0.26$. Regression statistics with other climate variables are given in Supporting Information S1: Table S5. PV, *Pinus virginiana*; PEC, *Pinus echinata*; PT1 and PT2, *Pinus taeda*; PEL, *Pinus elliottii*; PP, *P. palustris*.

Previous work on woody plants has shown a strong relationship between species' mean embolism resistance, indicated by the tension at which 50% of conductivity is lost ($P_{50}$), and the conduit double-wall-to-lumen-span ratio $(t/b)^2$ (Hacke et al. 2001; Domec, Warren, et al. 2009). In this study $(t/b)^2$, showed different correlations with other xylem anatomical and functional properties across organs. For example, in branches and roots, $(t/b)^2$ was strongly negatively associated with the mean conduit hydraulic diameter, but these correlations were not found in the needles (Figure 1a). The reason for correlations among anatomical properties involving $(t/b)^2$ to be present or absent depends, in part, on the variation among species in each contributing variable (provided as coefficient of variation in Supporting Information S1: Table S2). For example, in roots, the diameter-related variables and, even more, $(t/b)^2$ varied much more than $t$, while in leaves the variation was smaller. In addition, $(t/b)^2$ was strongly negatively associated with $K_{\text{s-xylem}}$ in branch, but these correlations were not found in leaves and roots (Figure 1a–c), indicating that assessments of the trade-off between hydraulic efficiency and safety must consider differences among organs. Moreover, $(t/b)^2$ showed high variation among organs, such that $(t/b)^2$ in branches was always higher than that in leaves and roots across species (Supporting Information S1: Table S1), indicating that branches are more resistant to cell wall implosion and embolism than leaves and roots (Choat et al. 2005; Johnson et al. 2011; McCulloh et al. 2019; Zhang et al. 2025). Higher $(t/b)^2$ in branches also makes them more resistant to mechanical stresses induced by gravity, wind and ice loading (Read and Stokes 2006; Domec et al. 2012). There was no difference in $(t/b)^2$ between leaves and roots, suggesting their comparable resistance to implosion under similar negative xylem pressure.

In terms of functional properties, the specific hydraulic conductivity of xylem, lumen and pits ($K_{\text{s-xylem}}$, $K_{\text{s-lumen}}$ and $K_{\text{s-pits}}$) decreased from roots to leaves (except in *P. palustris*, Supporting Information S1: Table S1). Leaf and branch hydraulic efficiency ($K_{\text{s-xylem}} = 1/R_{\text{s-xylem}}$) was determined by both $R_{\text{s-lumen}}$ and $R_{\text{s-pit}}$,

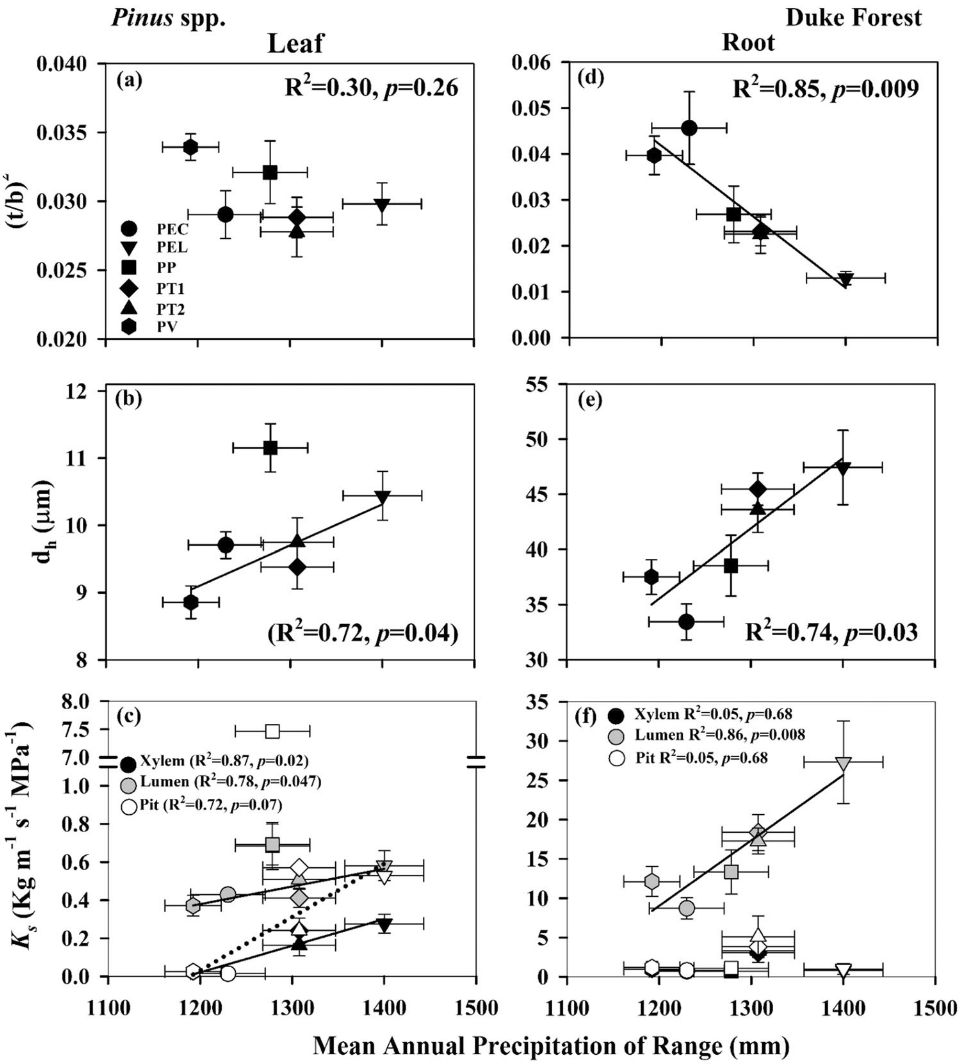

**FIGURE 7** | The response of anatomical and functional variables to increasing mean annual precipitation (MAP) of the native range in leaf (left panels) and root (right panels) of the five species studied. See Table 1 for definitions of variables. Note that roots have appreciably higher values for most variables. Note that statistics are given in parenthesis when *Pinus palustris* is excluded from the regression analysis; for statistics inclusive of that species see Supporting Information S1: Table S3. PV, *Pinus virginiana*; PEC, *Pinus echinata*; PT1 and PT2, *Pinus taeda*; PEL, *Pinus elliottii*; PP, *P. palustris*.

while root $R_{\text{s-xylem}}$ was mostly controlled by $R_{\text{s-pit}}$ (Figure 5), consistent with previous experimental and modelling studies on root hydraulic conductivity in conifers (Steudle and Peterson 1998; Domec et al. 2006). This difference seems to be caused by the variation in tracheid dimensions across organs. For example, $K_{\text{s-xylem}}$ showed positive correlations with tracheid diameter-related properties in needles and branches, but not in roots (Figure 1a–c). Roots had the largest tracheid diameter and root $K_{\text{s-lumen}}$ across organs (Supporting Information S1: Table S1), implying that the primary limitation for water transport in this organ occurred in the radial pathway ($K_{s\text{-pit}}$). Consequently, the species with the lowest root pit resistivity ($R_{\text{s-pits}}$), such as the two genotypes of *P. taeda* are likely to achieve the highest root $K_{s\text{-xylem}}$ (Supporting Information S1: Table S1).

In our study, we assumed that conduits were tubular in shape. We know that this approach is only an approximation, but most of the measured tracheids were circular with a few slightly oval, so we consider that this approach, extensively used in similar studies, did not exert large effect on the results (Tyree and Zimmermann 2002). We also assumed that the anatomical measurements performed in the middle section of the needle represented well the needle average values. Following Zwieniecki et al. (2006), we thus applied a correction factor of 0.96 to take into account the decline in either hydraulic diameter or $K_{\text{s-lumen}}$ with needle hydraulic path length. In conifer needles, we are not aware of studies that measured in detail the axial variation in conduit size and number with NL. Data from such anatomical investigations would help establish a more precise link between fine-scale anatomy and functionality.

## 4.2 | Xylem Hydraulic Differences Link to NL and the Climate of Natural Range

Previous work demonstrated that NL strongly influences needle anatomical traits, which, in turn, are reflected in leaf mechanical support, stomatal conductance and photosynthetic capacity

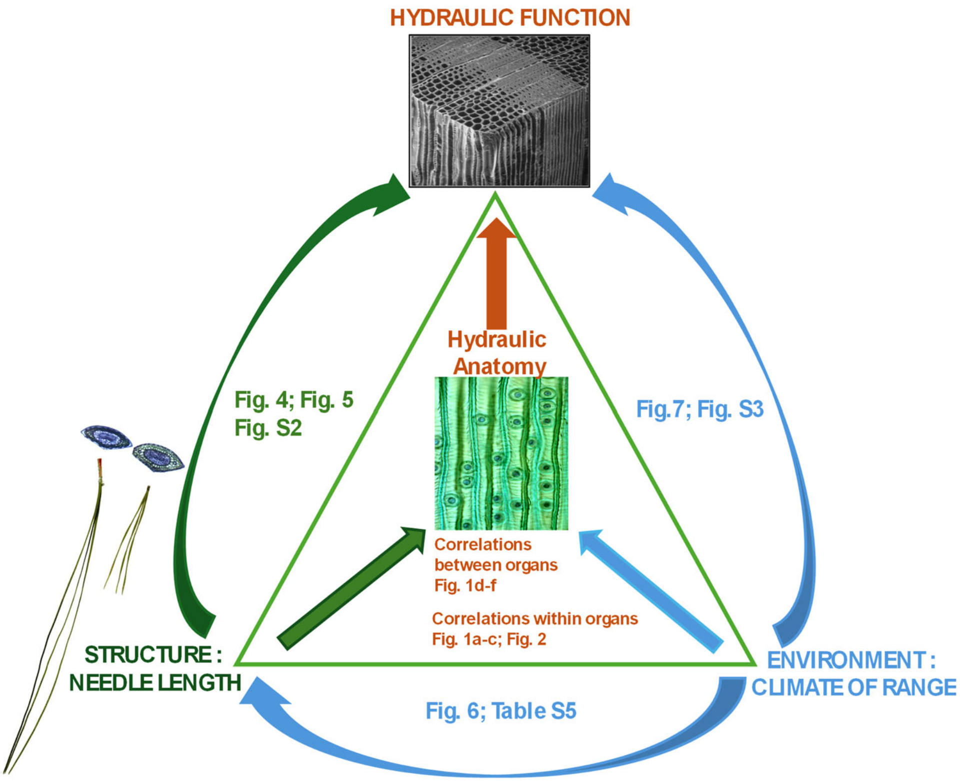

**FIGURE 8** | Integrated framework of whole-plant hydraulic strategy. The three corners of the triangle represent the three main axes of the whole-strategy approach in plant hydraulics, considering a plant as a multilevel organism and explicitly including the environmental dimension. It makes it possible to account for inter- and intra-organ trait variations, such as those in needle length (left corner of triangle) or between hydraulic function (top corner of triangle). Data (table or figure numbers) linking each triangle corner are also displayed. [Color figure can be viewed at wileyonlinelibrary.com]

(Kuusk et al. 2018; Wang et al. 2019). However, this study found a more striking pattern: leaf hydraulic anatomical and physiological traits exhibited even tighter correlations with NL than with mean climatic indices (MAP and MAT) representing CR of the five species (Figures 4a–c and 7a–c). This finding highlights a finer, functionally significant scale of variation that is more directly tied to NL.

In addition, only NL affected significantly the first PCA axis of leaf traits (Figure 3a), indicating that NL plays a key role in the overall structural design and function of needles, supporting our hypothesis **H2**. In support of our last hypothesis (**H3**), we found that certain xylem hydraulic properties, particularly of roots, varied with mean climatic indices representing CR of the five species (Figure 7d–f), even though all samples were obtained from trees growing at one site. Despite the relatively narrow range in MAP, species from regions with lower rainfall showed, as would be expected, higher root $(t/b)^2$, smaller root hydraulic diameter ($d_h$) and smaller $K_{\text{s-lumen}}$, implying higher resistance to embolism, and lower hydraulic efficiency, than those of wetter CR (Dickison 2000; Hacke et al. 2017). Although relationships were found with temperature-related variables in the native range, these were not as strong (Supporting Information S1: Table S3). It is noteworthy that root xylem hydraulic traits showed stronger correlations with CR than those of needles and branches. Roots, acting as the first sensors of soil water availability, may be more sensitive to dynamics of soil moisture than aboveground organs (Hacke et al. 2000; Domec et al. 2010; Lübbe et al. 2021). Finally, $(t/b)^2$ was negatively associated with $K_{\text{s-xylem}}$ in branches (Figure 1b). In turn, $K_s$ values were positively related to VPD (Supporting Information S1: Figure S3), in contrast to observation in *P. ponderosa* (Maherali and DeLucia 2000). We note, however, that the effect of VPD was principally caused by the lower VPD in the native range of *P. virginiana* and should be cautiously interpreted.

Nevertheless, measurements of water potential (Boroski et al. 2025) and vulnerability to embolism (Zhang et al. 2025) support a premise, consistent with Figure 7d,e, that roots of species with short needles (*P. virginiana* and *P echinata*) can bear more negative xylem pressure and be more resistant to negative xylem pressures with decreasing precipitation. The differences observed among the five pine species suggest differential susceptibility to warmer and/or dryer conditions. The genetic constraint on species hydraulic properties indicates that long-needle bearing species may not be able to acclimate to drier and hotter conditions. Small populations of montane longleaf pines are known to coexist with short-leaf and Virginia pines up to 600 m elevation (e.g., Pine Mountain, GA, USA), and it would be interesting to see if the anatomical and hydraulic traits in these populations are consistent with our results and our proposed integrated framework of whole-plant hydraulic strategy (Figure 8).

Our study points to strategies of root systems which should increase drought resistance through adjustment in root structure, leading to improved water transport capacity in some of the species; this variation may be a factor affecting the current and future distribution of these species. However, the role of these structural and functional differences in affecting actual water transport must be evaluated in the context of hydraulic traits of both the root system (e.g., rooting depth and area-density distribution) in relation to crown traits (e.g., leaf area).

## 4.3 | Partitioning of Resistivity in the Xylem

We found that, in the xylem hydraulic system from roots to leaves, the specific hydraulic resistivity partitioning between end-wall pits and lumen in leaves varied greatly among species (8%–99%), and that this variation was related to NL, in further support of hypothesis **H2** (Figure 5a). Leaf $\%R_{\text{s-pits}}/R_{\text{s-xylem}}$ decreased with NL, suggesting that more resistances are added in series in the longer axial water pathway of longer needles. The reasons for this could potentially be that there were more and/or larger pits per unit length in longer needles, leading to higher $K_{\text{s-pits}}$ and lower $R_{\text{s-pits}}$.

Roots had higher $\%R_{\text{s-pits}}/R_{\text{s-xylem}}$ than leaves and branches across species (Figure 5). Lancashire and Ennos (2002) demonstrated that tracheid resistance per length, normalised by cross-sectional area, is minimised when tracheid diameter increases with 2/3 power of the length, if the number of pits per area remains constant. In this case, the proportion of resistance residing in pits would be constant with respect to conduit size (Ooeda et al. 2018). At these optimal dimensions, pits should account for 67% of the total resistivity, which is close to the $\%R_{\text{s-pits}}/R_{\text{s-xylem}}$ in leaves and branches, but lower than $\%R_{\text{s-pits}}/R_{\text{s-xylem}}$ in roots measured in this and published studies (Domec et al. 2006). Therefore, only in the aboveground, tracheid diameter seems to be optimised to maximise conducting efficiency for a fixed tracheid length. Despite these variations, the average of $\%R_{\text{s-pits}}/R_{\text{s-xylem}}$ was always higher than that of $\%R_{\text{s-lumen}}/R_{\text{s-xylem}}$ in the xylem system across organs and species, meaning that the radial pathway is the primary site of limitation and regulation of water transport (Sperry et al. 2005). Taken together, pits play a major role in determining the efficiency of water transport through the xylem, and future work should incorporate more direct measurement of pit hydraulic characteristics across organs and species to provide greater insight into the sources of variation in plant hydraulic function.

In conclusion, the results suggest that NL and xylem structure and function are coordinated in a manner consistent with increasing hydraulic efficiency (Figure 8). These constraints may limit long-needled species to environments with sufficient moisture and milder climatic conditions, thereby influencing their biogeographic distribution. The five species studied here were planted at one site, eliminating variation that might be caused by growing in different climatic or edaphic conditions. Therefore, the relationship between root xylem hydraulic traits and species' CR provides evidence of a genetic control over the development of root xylem, which supports findings on pine embolism resistance across climate gradients (Lamy et al. 2014; López et al. 2016; Augustine and McCulloh 2024) The conservative nature of xylem traits in pine trees indicates that xylem anatomical and functional traits are not easily modified when growing in different climates. Collectively, our results provide new insight into whole tree hydraulic architecture and strategies and highlight the need for further research on the xylem physiological and structural adaptation mechanisms underlying species distributions.

## Acknowledgements

Na Wang gratefully acknowledges the financial support from the Scientific Research Project of Hunan Provincial Education Department (No.21B0642), and the Natural Science Foundation of Hunan Province (No. 2022JJ40012), and the Open Fund Project of Hunan Key Laboratory for Conservation and Utilization of Biological Resources in the Nanyue Mountainous Region (No.2021HSKFJJ036). Financial support for Ram Oren was provided by the Erkko Visiting Professor Programme of the Jane and Aatos Erkko 375th Anniversary Fund; additional support for Sari Palmroth and Ram Oren was provided by the ACCC Flagship – University of Helsinki, funded by the Academy of Finland (grant number 337549), both through the University of Helsinki. Some support was available from the Department of Energy, USA (No. DE-SC0023309), the Department of Defense, USA (SERDP RC-25-0189) and from the French ANR (grant PHYDRAUCC 21-CE02-0033-02) and the Nlle Aquitaine Region (Project VITIPIN AAPR2020-2020-8596610, GRIFFON and IMPACTS). We thank NC State University Cooperative Tree Improvement Program and the USDA Forest Service for access to the Longleaf Pine Regional Provenance/Progeny Trial at Duke Forest.

## Data Availability Statement

The data that support the findings of this study are available from the corresponding author upon reasonable request.

## References

Anfodillo, T., G. Petit, and A. Crivellaro. 2013. "Axial Conduit Widening in Woody Species: A Still Neglected Anatomical Pattern." *IAWA Journal* 34: 352–364.

Augustine, S. P., and K. A. McCulloh. 2024. "Physiological Trait Coordination and Variability Across and Within Three *Pinus* Species." *New Phytologist* 244: 451–463.

Becker, P., R. J. Gribben, and P. J. Schulte. 2003. "Incorporation of Transfer Resistance Between Tracheary Elements Into Hydraulic Resistance Models for Tapered Conduits." *Tree Physiology* 23: 1009–1019.

Bonetti, S., D. Breitenstein, S. Fatichi, J. C. Domec, and D. Or. 2021. "Persistent Decay of Fresh Xylem Hydraulic Conductivity Varies With Pressure Gradient and Marks Plant Responses to Injury." *Plant Cell & Environment* 44: 371–386. https://doi.org/10.1111/pce.13893.

Booker, R. E. 1977. "Problems in the Measurement of Longitudinal Sapwood Permeability and Hydraulic Conductivity." *New Zealand Journal of Forest Science* 7: 297–306.

Boroski, C. A., J. C. Domec, C. A. Maier, S. Palmroth, Y. Wang, and R. Oren. 2025. "Leaf Transpiration Decreases Similarly Among Five Pine Species as Height Increases Over Stand Development." *Tree Physiology*. In press.

Bouche, P. S., M. Larter, J. C. Domec, et al. 2014. "A Broad Survey of Hydraulic and Mechanical Safety in the Xylem of Conifers." *Journal of Experimental Botany* 65: 4419–4431.

Brodribb, T. J., S. A. M. McAdam, G. J. Jordan, and S. C. V. Martins. 2014. "Conifer Species Adapt to Low-Rainfall Climates by Following One of Two Divergent Pathways." *Proceedings of the National Academy of Sciences of the United States of America* 111: 14489–14493.

Charra-Vaskou, K., and S. Mayr. 2011. "The Hydraulic Conductivity of the Xylem in Conifer Needles (*Picea abies* and *Pinus mugo*)." *Journal of Experimental Botany* 62: 4383–4390.

Choat, B., E. C. Lahr, P. J. Melcher, M. A. Zwieniecki, and N. M. Holbrook. 2005. "The Spatial Pattern of Air Seeding Thresholds in Mature Sugar Maple Trees." *Plant, Cell & Environment* 28: 1082–1089.

Cochard, H., A. Nardini, and L. Coll. 2004. "Hydraulic Architecture of Leaf Blades: Where is the Main Resistance?" *Plant, Cell & Environment* 27: 1257–1267.

Creek, D., C. J. Blackman, T. J. Brodribb, B. Choat, and D. T. Tissue. 2018. "Coordination Between Leaf, Stem, and Root Hydraulics and Gas Exchange in Three Arid-Zone Angiosperms During Severe Drought and Recovery." *Plant, Cell & Environment* 41: 2869–2881.

Delucia, E. H., H. Maherali, and E. V. Carey. 2000. "Climate-Driven Changes in Biomass Allocation in Pines." *Global Change Biology* 6, no. 5: 587–593.

Dickison, W. C. 2000. *Integrative Plant Anatomy*. Academic Press.

Domec, J. C., B. Lachenbruch, and F. C. Meinzer. 2006. "Bordered Pit Structure and Function Determine Spatial Patterns of Air-Seeding Thresholds in Xylem of Douglas-Fir (*Pseudotsuga menziesii*; Pinaceae) Trees." *American Journal of Botany* 93: 1588–1600.

Domec, J. C., B. Lachenbruch, F. C. Meinzer, D. R. Woodruff, J. M. Warren, and K. A. McCulloh. 2008. "Maximum Height in a Conifer Is Associated With Conflicting Requirements for Xylem Design." *Proceedings of the National Academy of Sciences of the United States of America* 105: 12069–12074.

Domec, J. C., B. Lachenbruch, M. L. Pruyn, and R. Spicer. 2012. "Effects of Age-Related Increases in Sapwood Area, Leaf Area, and Xylem Conductivity on Height-Related Hydraulic Costs in Two Contrasting Coniferous Species." *Annals of Forest Science* 69: 17–27. https://doi.org/10.1007/s13595-011-0154-3.

Domec, J.-C., A. Noormets, J. S. King, et al. 2009. "Decoupling the Influence of Leaf and Root Hydraulic Conductances on Stomatal Conductance and Its Sensitivity to Vapor Pressure Deficit as Soil Dries in a Drained Loblolly Pine Plantation." *Plant, Cell and Environment* 32: 980–991.

Domec, J. C., S. Palmroth, and R. Oren. 2016. "Effects of *Pinus taeda* Leaf Anatomy on Vascular and Extravascular Leaf Hydraulic Conductance as Influenced by N-Fertilization and Elevated $CO_2$." *Journal of Plant Hydraulics* 3: e007.

Domec, J. C., K. Schafer, R. Oren, H. S. Kim, and H. R. McCarthy. 2010. "Variable Conductivity and Embolism in Roots and Branches of Four Contrasting Tree Species and Their Impacts on Whole-Plant Hydraulic Performance Under Future Atmospheric $CO_2$ Concentration." *Tree Physiology* 30: 1001–1015.

Domec, J. C., J. M. Warren, F. C. Meinzer, and B. Lachenbruch. 2009. "Safety Factors for Xylem Failure by Implosion and Air-Seeding Within Roots, Trunks and Branches of Young and Old Conifer Trees." *IAWA Journal* 30: 101–120.

Duboscq-Carra, V. G., J. A. Arias-Rios, V. A. El Mujtar, P. Marchelli, and M. J. Pastorino. 2020. "Differentiation in Phenology Among and Within Natural Populations of a South American Nothofagus Revealed by a Two-Year Evaluation in a Common Garden Trial." *Forest Ecology and Management* 460: 117858.

Dunham, S. M., B. Lachenbruch, and L. M. Ganio. 2006. "Bayesian Analysis of Douglas-Fir Hydraulic Architecture at Multiple Scales." *Trees* 21: 65–78.

Ewers, B. E., R. Oren, and J. S. Sperry. 2000. "Influence of Nutrient Versus Water Supply on Hydraulic Architecture and Water Balance in *Pinus taeda*." *Plant, Cell & Environment* 23: 1055–1066.

Gleason, S. M., C. J. Blackman, S. T. Gleason, K. A. McCulloh, T. W. Ocheltree, and M. Westoby. 2018. "Vessel Scaling in Evergreen Angiosperm Leaves Conforms With Murray's Law and Area-Filling Assumptions: Implications for Plant Size, Leaf Size and Cold Tolerance." *New Phytologist* 218: 1360–1370.

Hacke, U. G., J. S. Sperry, B. E. Ewers, D. S. Ellsworth, K. V. R. Schäfer, and R. Oren. 2000. "Influence of Soil Porosity on Water Use in *Pinus taeda*." *Oecologia* 124: 495–505.

Hacke, U. G., J. S. Sperry, W. T. Pockman, S. D. Davis, and K. A. McCulloh. 2001. "Trends in Wood Density and Structure Are Linked to Prevention of Xylem Implosion by Negative Pressure." *Oecologia* 126: 457–461.

Hacke, U. G., R. Spicer, S. G. Schreiber, and L. Plavcová. 2017. "An Ecophysiological and Developmental Perspective on Variation in Vessel Diameter." *Plant, Cell & Environment* 40: 831–845.

He, P., S. M. Gleason, I. J. Wright, et al. 2020. "Growing-Season Temperature and Precipitation Are Independent Drivers of Global Variation in Xylem Hydraulic Conductivity." *Global Change Biology* 26: 1833–1841.

Jankowski, A., T. P. Wyka, R. Żytkowiak, D. Danusevičius, and J. Oleksyn. 2019. "Does Climate-Related In Situ Variability of Scots Pine (*Pinus sylvestris* L.) Needles Have a Genetic Basis? Evidence From Common Garden Experiments." *Tree Physiology* 39: 573–589.

Johnson, D. M., K. A. McCulloh, F. C. Meinzer, D. R. Woodruff, and D. M. Eissenstat. 2011. "Hydraulic Patterns and Safety Margins, From Stem to Stomata, in Three Eastern US Tree Species." *Tree Physiology* 31: 659–668.

Johnson, D. M., R. Wortemann, K. A. McCulloh, et al. 2016. "A Test of the Hydraulic Vulnerability Segmentation Hypothesis in Angiosperm and Conifer Tree Species." *Tree Physiology* 36: 983–993.

Kilgore, J. S., A. L. Jacobsen, and F. W. Telewski. 2021. "Hydraulics of *Pinus* (Subsection Ponderosae) Populations Across an Elevation Gradient in the Santa Catalina Mountains of Southern Arizona." *Madroño* 67: 218–226.

Koch, G. W., S. C. Sillett, G. M. Jennings, and S. D. Davis. 2004. "The Limits to Tree Height." *Nature* 428: 851–854.

Kuusk, V., Ü. Niinemets, and F. Valladares. 2018. "A Major Trade-Off Between Structural and Photosynthetic Investments Operative Across Plant and Needle Ages in Three Mediterranean Pines." *Tree Physiology* 38: 543–557.

Lamy, J. B., S. Delzon, P. S. Bouche, et al. 2014. "Limited Genetic Variability and Phenotypic Plasticity Detected for Cavitation Resistance in a Mediterranean Pine." *New Phytologist* 201: 874–886.

Lancashire J. R., and A. R. Ennos. 2002. "Modelling the Hydrodynamic Resistance of Bordered Pits." *Journal of Experimental Botany* 53: 1485–1493. https://doi.org/10.1093/jexbot/53.373.1485.

Lazzarin, M., A. Crivellaro, C. B. Williams, T. E. Dawson, G. Mozzi, and T. Anfodillo. 2016. "Tracheid and Pit Anatomy Vary in Tandem in a Tall *Sequoiadendron giganteum* Tree." *IAWA Journal* 37: 172–185.

Lechthaler, S., P. Colangeli, M. Gazzabin, and T. Anfodillo. 2019. "Axial Anatomy of the Leaf Midrib Provides New Insights Into the Hydraulic Architecture and Cavitation Patterns of *Acer pseudoplatanus* Leaves." *Journal of Experimental Botany* 70: 6195–6201.

Li, X., C. J. Blackman, B. Choat, et al. 2018. "Tree Hydraulic Traits Are Coordinated and Strongly Linked to Climate-of-Origin Across a Rainfall Gradient." *Plant, Cell & Environment* 41: 646–660.

Liu, H., Q. Ye, S. M. Gleason, P. He, and D. Yin. 2021. "Weak Tradeoff Between Xylem Hydraulic Efficiency and Safety: Climatic Seasonality Matters." *New Phytologist* 229: 1440–1452.

López, R., F. J. Cano, B. Choat, H. Cochard, and L. Gil. 2016. "Plasticity in Vulnerability to Cavitation of *Pinus canariensis* Occurs Only at the Driest End of an Aridity Gradient." *Frontiers in Plant Science* 7: 769.

Lübbe, T., L. J. Lamarque, S. Delzon, et al. 2021. "High Variation in Hydraulic Efficiency but Not Xylem Safety Between Roots and Branches in Four Temperate Broad-Leaved Tree Species." *Functional Ecology* 3: 699–712.

Luo, D., C. Wang, Y. Jin, Z. Li, and Z. Wang. 2023. "Different Hydraulic Strategies Under Drought Stress Between *Fraxinus mandshurica* and

*Larix gmelinii* Seedlings." *Journal of Forestry Research* 34: 99–111. https://doi.org/10.1007/s11676-021-01438-1.

Maherali, H., and E. H. DeLucia. 2000. "Xylem Conductivity and Vulnerability to Cavitation of Ponderosa Pine Growing in Contrasting Climates." *Tree Physiology* 20: 859–867.

Maurel, C., and P. Nacry. 2020. "Root Architecture and Hydraulics Converge for Acclimation to Changing Water Availability." *Nature Plants* 6: 744–749.

McCulloh, K., J. S. Sperry, B. Lachenbruch, F. C. Meinzer, P. B. Reich, and S. Voelker. 2010. "Moving Water Well: Comparing Hydraulic Efficiency in Twigs and Trunks of Coniferous, Ring-Porous, and Diffuse-Porous Saplings From Temperate and Tropical Forests." *New Phytologist* 186: 439–450.

McCulloh, K. A., J. C. Domec, D. M. Johnson, D. D. Smith, and F. C. Meinzer. 2019. "A Dynamic Yet Vulnerable Pipeline: Integration and Coordination of Hydraulic Traits Across Whole Plants." *Plant, Cell & Environment* 42: 2789–2807.

McCulloh, K. A., and J. S. Sperry. 2005. "Patterns in Hydraulic Architecture and Their Implications for Transport Efficiency." *Tree Physiology* 25: 257–267.

Melcher, P. J., N. Michele Holbrook, M. J. Burns, et al. 2012. "Measurements of Stem Xylem Hydraulic Conductivity in the Laboratory and Field." *Methods in Ecology and Evolution* 3: 685–694.

Nardini, A., E. Gortan, and S. Salleo. 2005. "Hydraulic Efficiency of the Leaf Venation System in Sun- and Shade-Adapted Species." *Functional Plant Biology* 32: 953–961.

Ooeda, H., I. Terashima, and H. Taneda. 2018. "Intra-Specific Trends of Lumen and Wall Resistivities of Vessels Within the Stem Xylem Vary Among Three Woody Plants." *Tree Physiology* 38: 223–231.

Petit, G., F. A. J. DeClerck, M. Carrer, and T. Anfodillo. 2014. "Axial Vessel Widening in Arborescent Monocots." *Tree Physiology* 34: 137–145.

Pfautsch, S., M. J. Aspinwall, J. E. Drake, et al. 2018. "Traits and Trade-Offs in Whole-Tree Hydraulic Architecture Along the Vertical Axis of *Eucalyptus grandis*." *Annals of Botany* 121: 129–141.

Pittermann, J., and J. S. Sperry. 2006. "Analysis of Freeze-Thaw Embolism in Conifers. The Interaction Between Cavitation Pressure and Tracheid Size." *Plant Physiology* 140: 374–382.

Pittermann, J., J. S. Sperry, J. K. Wheeler, U. G. Hacke, and E. H. Sikkema. 2006. "Mechanical Reinforcement of Tracheids Compromises the Hydraulic Efficiency of Conifer Xylem." *Plant, Cell & Environment* 29: 1618–1628.

Pockman, W. T., and J. S. Sperry. 2000. "Vulnerability to Xylem Cavitation and the Distribution of Sonoran Desert Vegetation." *American Journal of Botany* 87: 1287–1299.

Pritzkow, C., V. Williamson, C. Szota, R. Trouvé, and S. K. Arndt. 2020. "Phenotypic Plasticity and Genetic Adaptation of Functional Traits Influences Intra-Specific Variation in Hydraulic Efficiency and Safety." *Tree Physiology* 40: 215–229.

R Core Team. 2019. R: A Language and Environment for Statistical Computing. R Foundation for Statistical Computing. https://www.R-project.org/.

Read, J., and A. Stokes. 2006. "Plant Biomechanics in an Ecological Context." *American Journal of Botany* 93: 1546–1565.

Rosas, T., M. Mencuccini, J. Barba, H. Cochard, S. Saura-Mas, and J. Martínez-Vilalta. 2019. "Adjustments and Coordination of Hydraulic, Leaf and Stem Traits Along a Water Availability Gradient." *New Phytologist* 223: 632–646.

Rosner, S., A. Klein, U. Muller, and B. Karlsson. 2007. "Hydraulic and Mechanical Properties of Young Norway Spruce Clones Related to Growth and Wood Structure." *Tree Physiology* 27: 1165–1178.

Sack, L., C. M. Streeter, and N. M. Holbrook. 2004. "Hydraulic Analysis of Water Flow Through Leaves of Sugar Maple and Red Oak." *Plant Physiology* 134: 1824–1833.

Schuldt, B., C. Leuschner, N. Brock, and V. Horna. 2013. "Changes in Wood Density, Wood Anatomy and Hydraulic Properties of the Xylem Along the Root-to-Shoot Flow Path in Tropical Rainforest Trees." *Tree Physiology* 33: 161–174.

Schulte, P. J., U. G. Hacke, and A. L. Schoonmaker. 2015. "Pit Membrane Structure Is Highly Variable and Accounts for a Major Resistance to Water Flow Through Tracheid Pits in Stems and Roots of Two Boreal Conifer Species." *New Phytologist* 208: 102–113.

Soriano, D., A. Echeverría, T. Anfodillo, J. A. Rosell, and M. E. Olson. 2020. "Hydraulic Traits Vary as the Result of Tip-to-Base Conduit Widening in Vascular Plants." *Journal of Experimental Botany* 71: 4232–4242.

Sperry, J. S., U. G. Hacke, and J. Pittermann. 2006. "Size and Function in Conifer Tracheids and Angiosperm Vessels." *American Journal of Botany* 93: 1490–1500.

Sperry, J. S., U. G. Hacke, and J. K. Wheeler. 2005. "Comparative Analysis of End Wall Resistivity in Xylem Conduits." *Plant, Cell & Environment* 28: 456–465.

Steudle, E., and C. A. Peterson. 1998. "How Does Water Get Through Roots?" *Journal of Experimental Botany* 49: 775–788.

Trabucco, A., and R. J. Zomer. 2009. *Global Aridity Index (Global-Aridity) and Global Potential Evapo-Transpiration (Global-PET) Geospatial Database*. CGIAR Consortium for Spatial Information. http://www.csi.cgiar.org.

Tsuda, M., and M. T. Tyree. 2000. "Plant Hydraulic Conductance Measured by the High Pressure Flow Meter in Crop Plants." *Journal of Experimental Botany* 51: 823–828.

Tyree, M. T., and F. W. Ewers. 1991. "The Hydraulic Architecture of Trees and Other Woody Plants." *New Phytologist* 119: 345–360.

Tyree, M. T., S. Patiño, J. Bennink, and J. Alexander. 1995. "Dynamic Measurements of Roots Hydraulic Conductance Using a High-Pressure Flowmeter in the Laboratory and Field." *Journal of Experimental Botany* 46: 83–94.

Tyree, M. T., and M. H. Zimmermann. 2002. *Xylem Structure and the Ascent of Sap*, 284. Springer.

Wang, N., S. Palmroth, C. A. Maier, J. C. Domec, and R. Oren. 2019. "Anatomical Changes With Needle Length Are Correlated With Leaf Structural and Physiological Traits Across Five *Pinus* Species." *Plant, Cell & Environment* 42: 1690–1704.

Wang, Y. 2021. *Carbon Gain and Allocation in Five Shade Intolerant* Pinus *Species*. Duke University. https://hdl.handle.net/10161/24058.

Zhang, H., J. C. Domec, C. A. Maier, et al. 2025. "Similar Response of Canopy Conductance to Increasing Vapor Pressure Deficit and Decreasing Soil Conductivity With Drought Among Five Co-Occurring Pine Species of a Large Range in Crown Architecture." *Agricultural Forest Meteorology* 366: 110479.

Zotz, G., M. T. Tyree, and M. R. Carlton. 1998. "Hydraulic Architecture and Water Use of Selected From a Lower Montane Forest in Panama." *Trees* 477: 1–8.

Zwieniecki, M. A. 2004. "Functional Design Space of Single-Veined Leaves: Role of Tissue Hydraulic Properties in Constraining Leaf Size and Shape." *Annals of Botany* 94: 507–513.

Zwieniecki, M. A., H. A. Stone, A. Leigh, C. K. Boyce, and N. M. Holbrook. 2006. "Hydraulic Design of Pine Needles: One Dimensional Optimization for Single-Vein Leaves." *Plant, Cell & Environment* 29: 803–809.

## Supporting Information

Additional supporting information can be found online in the Supporting Information section.